3D modeling of ground rupture in thrust and reverse fault earthquakes: A distinct element approach

Kristen Chiama, Andreas Plesch, John H. Shaw
Harvard University, Cambridge MA, USA.
Contact: kchiama@g.harvard.edu

Abstract

Thrust and reverse fault scarps that form during large earthquakes often feature complex patterns of distributed folding, fracturing, and uplift in surface fault ruptures that can vary significantly along-strike. We aim to evaluate the influence of fault parameters (slip, dip) and sediment strength mechanics on the patterns of ground surface deformation. We produced 80 3D distinct element method (DEM) models across 4 case studies: 1, planar faults with constant fault dip (20º, 40º, 60º); 2, variable fault dip along-strike from 20º to 70º; 3, variable depth of the fault tip; 4, amount of obliquity in fault slip. Across all of these cases, we tested homogeneous and heterogeneous sediment strengths by modifying the cohesion of the contact bonds using the parallel-bond contact model. We tested homogeneous sediment strengths including weak (1 MPa), moderate (3 MPa), and strong (5 MPa) sediment as well as heterogeneous sediment conditions with randomized heterogeneities along-strike and a cohesive top unit above loosely consolidated sediment.

Our results show that the most influential factor in determining the overall scarp type is the near-surface fault dip. Shallow faults produce pressure ridge scarps while steep faults produce monoclinal or simple scarps (consistent with Chiama et al., 2023, 2025). In parallel, the sediment strength determines the localization of slip in the near surface and differentiates the formation of monoclinal and simple scarps. The models with fault dip variability have the most diversity in scarp types present, while the randomized heterogeneity in sediment strength and depth of the fault tip produces the variability in surface deformation characteristics (scarp height, deformation zone width, scarp dip) within the given scarp type. Thus, the fault dip and along-strike variability in sediment strengths both contribute to significant along-strike variability in fault scarp morphology. We propose that insights from these 3D DEM models can help inform local site assessments for seismic hazards and aid in the community efforts for Probabilistic Fault Displacement Hazard Assessments (PFDHA).

Introduction & Methodology

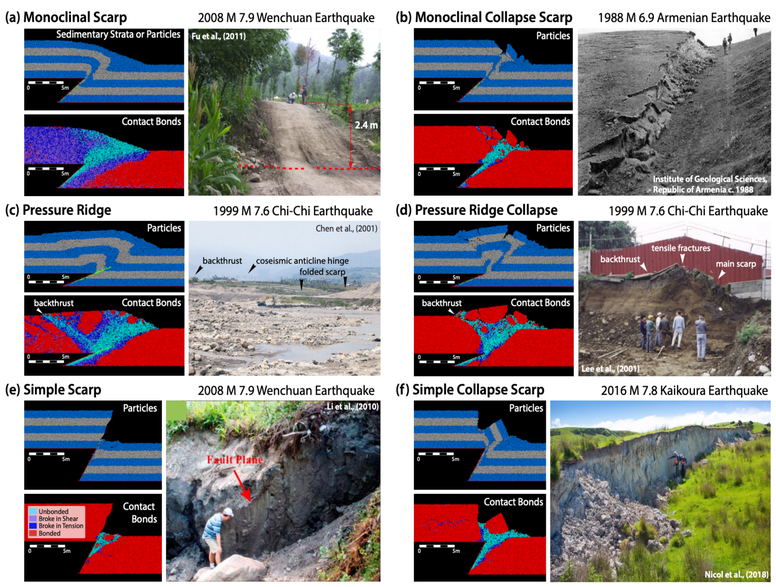

Fig. 1. Patterns of scarp morphologies for thrust and reverse faults, modified from Chiama et al. (2023). (a) Monoclinal scarp, (b) monoclinal collapse-modified scarp, (c) pressure ridge scarp, (d) pressure ridge collapse-modified scarp, (e) simple scarp, (f) simple collapse-modified scarp.

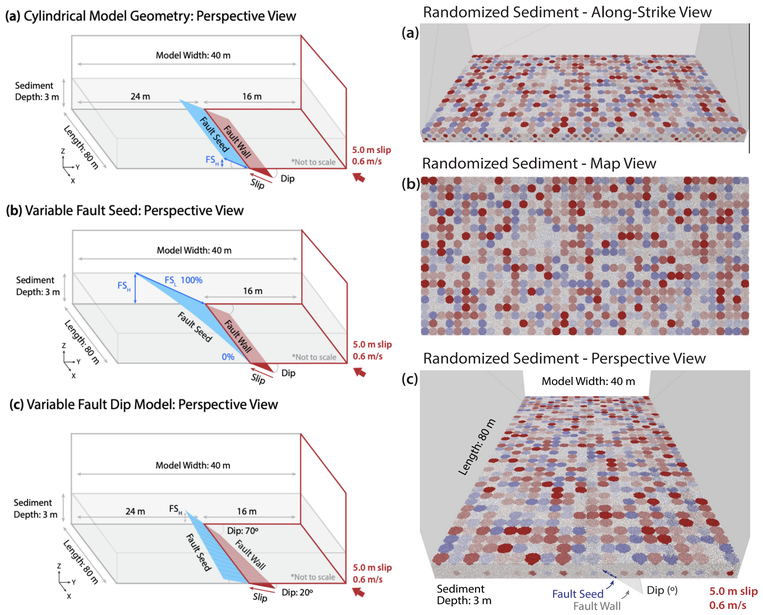

Fig. 2. 3D DEM model geometries. (a) Cylindrical model geometry for a planar fault with constant dip. (b) variable fault seed model geometry with a planar fault of constant dip in perspective view. (c) Model geometry with variable fault dip along-strike from 20º to 70º in 1º increments. The sediment is represented as 3D light grey shading. The fault wall is shaded in dark red underneath the sediment. The hanging wall is outlined in dark red and slips at a rate of 0.6 m/s for a total of 5.0 m at the specified fault dip. The fault seed is represented as bright blue, propagating a plane of weakness at the fault dip angle into the sediment above the tip of the fault wall.

Fig. 3. 3D DEM model initial state for randomized contact bond strengths for the (a) along-strike, (b) map, and (c) perspective views respectfully. Random contact bond spheres are 1.0 m or 0.5 m radii in a lattice throughout the model domain and the cohesion and tensile strength of the contact bonds are applied through a random number generator between 1 MPa (weak sediment) to 6 MPa (strong sediment).

Results

Planar Fault Model

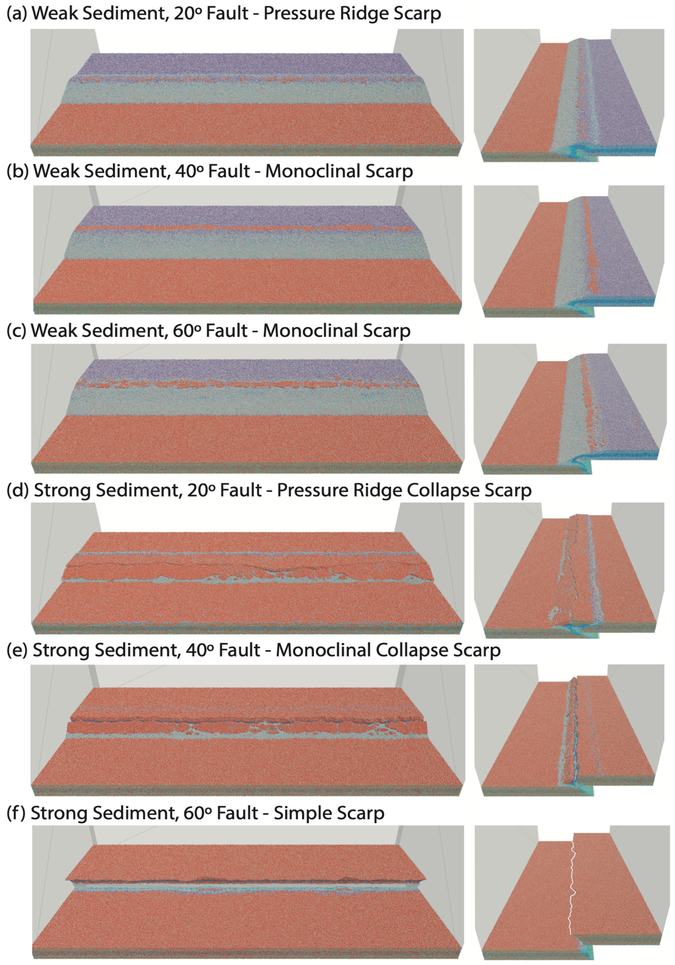

Variable Fault Dip Model

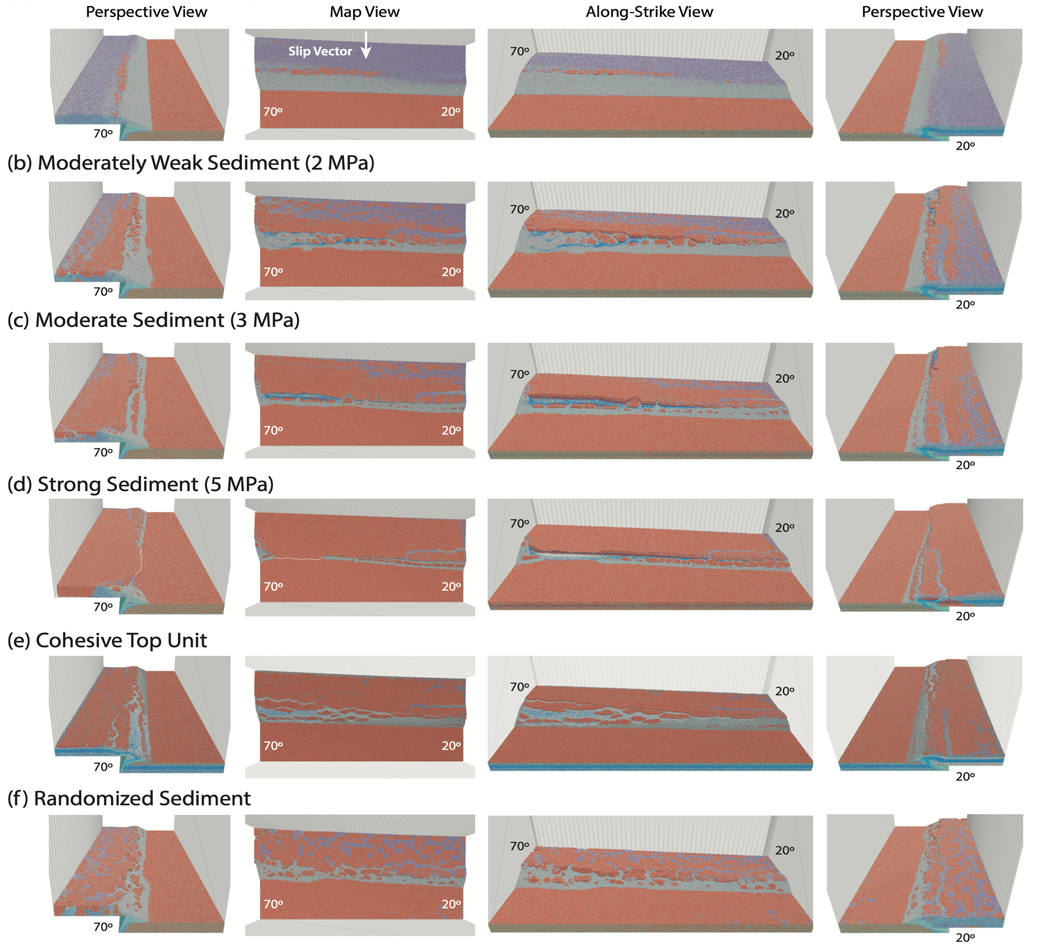

Planar Fault Model - Random Sediment

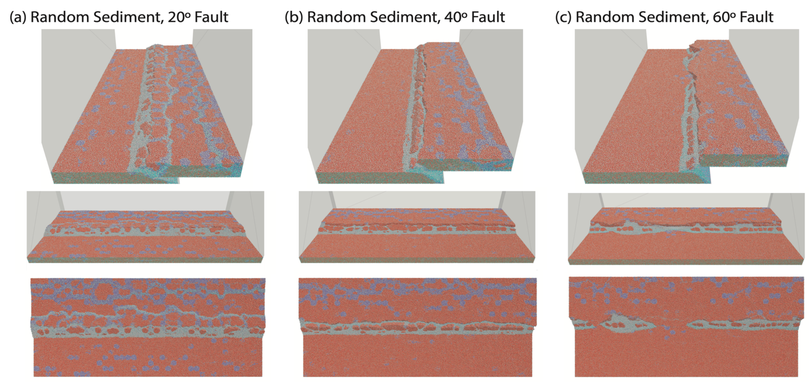

Planar Fault Model - Variable Fault Seed

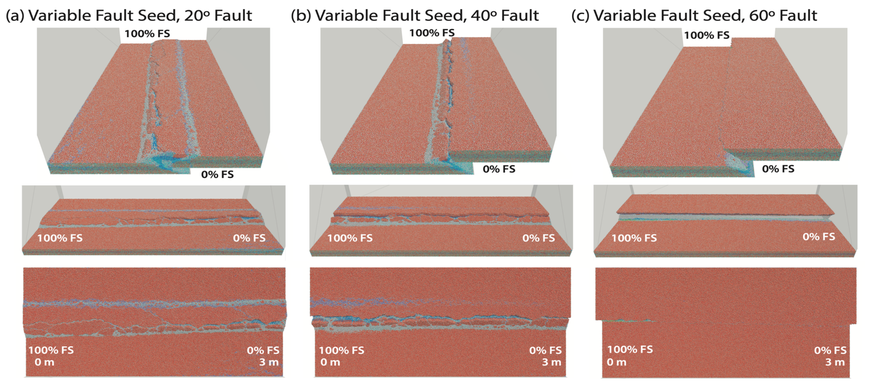

Data Analysis

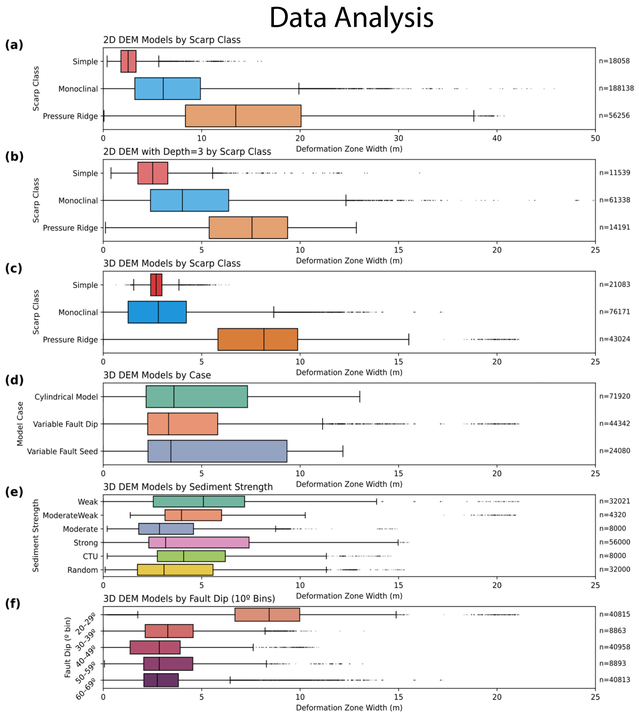

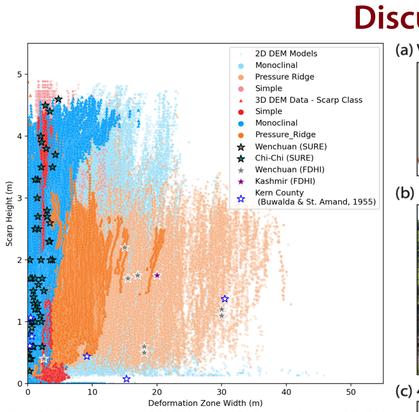

Fig. 8. Comparison of 2D DEM model measurements for the deformation zone width from Chiama et al. (2025) to 3D DEM models. (a) Full range of 2D DEM model measurements by scarp class. Scale is up to 50 m wide. (b) Only 3m sediment depth 2D DEM models by scarp class. Scale is up to 25 m wide. (c) All 3D DEM model measurements by scarp class. (d) 3D DEM model measurements organized by case and fault geometry. (e) 3D DEM model measurements organized by sediment strength. CTU: Cohesive top unit. (f) 3D DEM model measurements organized by fault dip. Boxplots depict quartiles, outliers are small dots.

Fig. 9. Comparison of 3D DEM model results to the 2D DEM models results from Chiama et al. (2025) and historical earthquakes from the FDHI (Sarmiento et al., 2024) and SURE (Nurminen et al., 2022) datasets. 2D DEM data from Chiama et al. (2025) lightly shaded by scarp class in the background. 3D DEM data shown in triangles and bold colors by scarp class in the foreground. SURE dataset events are stars with a black border. FDHI dataset events are stars with a white border. Measurements from 1952 M 7.36 Kern County presented in Buwalda & St. Amand (1955) are white stars with a blue border.

Discussion & Conclusions

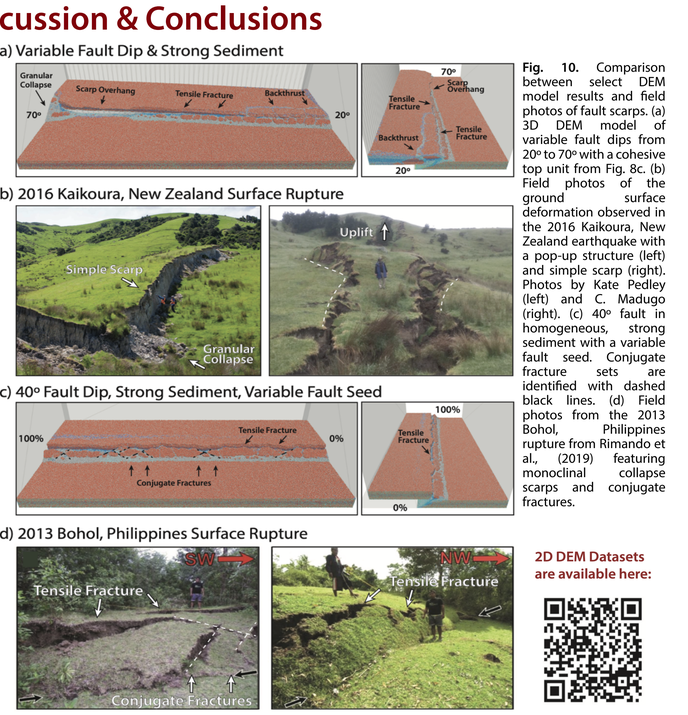

Fig. 10. Comparison between select DEM model results and field photos of fault scarps. (a) 3D DEM model of variable fault dips from 20º to 70º with a cohesive top unit from Fig. 8c. (b) Field photos of the ground surface deformation observed in the 2016 Kaikoura, New Zealand earthquake with a pop-up structure (left) and simple scarp (right). Photos by Kate Pedley (left) and C. Madugo (right). (c) 40º fault in homogeneous, strong sediment with a variable fault seed. Conjugate fracture sets are identified with dashed black lines. (d) Field photos from the 2013 Bohol, Philippines rupture from Rimando et al., (2019) featuring monoclinal collapse scarps and conjugate fractures.

2D DEM Datasets are available here:

References

1. Baize, S. et al., 2019, A worldwide and unified database of surface ruptures (SURE) for fault displacement hazard analyses: Seismological Research Letters, v. 91, p. 499–520, doi:10.1785/0220190144.
2. Boncio, P., Liberi, F., Caldarella, M., and Nurminen, F.C., 2018, Width of surface rupture zone for thrust earthquakes: Implications for earthquake fault zoning: Natural Hazards and Earth System Sciences, v. 18, p. 241–256, doi:10.5194/nhess-18-241-2018.
3. Chiama, K., A. Plesch, J. Shaw. (2025) 3D Distinct Element Method (DEM) Models of Ground Surface Deformation Associated with Thrust and Reverse Fault Earthquakes. DesignSafe-CI. doi: 10.17603/ds2-xgqp-ay07; 10.17603/ds2-zt8x-6e73; 10.17603/ds2-8kb3-5g63.
4. Chiama K, Bednarz W, Moss R, Plesch A, Shaw JH, 2025, Quantifying relationships between fault parameters and rupture characteristics associated with thrust and reverse fault earthquakes. Earthquake Spectra, 2025;0(0). doi:10.1177/87552930251346434
5. Chiama, K., Chauvin, B., Plesch, A., Moss, R., and Shaw, J.H., 2023, Geomechanical Modeling of Ground Surface Deformation Associated with Thrust and Reverse-Fault Earthquakes: A Distinct Element Approach: Bulletin of the Seismological Society of America, doi:10.1785/0120220264.
6. Garcia, F.E., and Bray, J.D., 2018a, Distinct element simulations of earthquake fault rupture through materials of varying density: Soils and Foundations, v. 58, p. 986–1000, doi:10.1016/j.sandf.2018.05.009.
7. Garcia, F.E., and Bray, J.D., 2018b, Distinct Element Simulations of Shear Rupture in Dilatant Granular Media: International Journal of Geomechanics, v. 18, p. 04018111, doi:10.1061/(asce)gm.1943-5622.0001238.
8. Garcia, F.E., & Bray, J.D. (2022). Discrete element analysis of earthquake surface fault rupture through layered media. Soil Dynamics and Earthquake Engineering, 152, 107021. https://doi.org/10.1016/j.soildyn.2021.107021
9. Nurminen, F., Baize, S., Boncio, P. et al. SURE 2.0 – New release of the worldwide database of surface ruptures for fault displacement hazard analyses. Sci Data 9, 729 (2022). https://doi.org/10.1038/s41597-022-01835-z
10. Sarmiento A, Madugo D, Shen A, et al., 2024, Database for the Fault Displacement Hazard Initiative Project. Earthquake Spectra, v. 0(0). doi:10.1177/87552930241262766.
11. Rimando, J.M., Aurelio, M.A., Dianala, J.D.B., Taguibao, K.J.L., Agustin, K.M.C., Berador, A.E.G., and Vasquez, A.A., 2019, Coseismic Ground Rupture of the 15 October 2013 Magnitude (MW) 7.2 Bohol Earthquake, Bohol Island, Central Philippines: Tectonics, v. 38, p. 2558–2580, doi:10.1029/2019TC005503.

Acknowledgments

This research was supported by the National Science Foundation (NSF), Division of Earth Sciences (EAR), Tectonics Program, Grant Number 2207119; and by the Southern California Earthquake Center (SCEC) Agreement Number 110862181 (SCEC Award Number 22013). We thank F. Estefan Garcia, Curtis Baden, Benjamin Chauvin, Brendan Meade, Emily Carrero Mustelier, Brook Runyon, Lluis Salo-Salgado, Natasha Toghramadjian, and Robert Welch for thoughtful discussions and coding suggestions.